CAPTURE VELOCITY WITH SLOT ENTRY TO CONICAL HOOD

by

Matthew Lucas Hibbs

A thesis submitted in partial fulfillment of the requirements for the Master of Science degree in Occupational and Environmental Health in the Graduate College of The University of Iowa

July 2011

Thesis Supervisor: Assistant Professor T. Renée Anthony

Graduate College
The University of Iowa
Iowa City, Iowa

CERTIFICATE OF APPROVAL

MASTER'S THESIS

This is to certify that the Master's thesis of

Matthew Lucas Hibbs

has been approved by the Examining Committee for the thesis requirement for the Master of Science degree in Occupational and Environmental Health at the July 2011 graduation.

Thesis Committee: ______________________________

T. Renée Anthony, Thesis Supervisor

____

Patrick O'Shaughnessy

____

Thomas Peters

To my family, thank you for all your support.

ACKNOWLEDGMENTS

I would like to thank my advisor T. Renée Anthony for the support and guidance it took to make this thesis possible. I would also like to thank Tom Peters and Patrick O'Shaughnessy for their help with edits and evolving this work. I want to thank the organization that provided funding for this research and my education: CDC/NIOSH Education and Research Center Training Grant (T42OH008491). Finally, I would like to thank all my friends and colleagues at IREH. Thank you.

ABSTRACT

The objective of this study was to determine whether improvements could be made to increase the capture distance of traditional local exhaust ventilation (LEV) hoods by designing a circular slotted-hood. The criterion of success for this study was to achieve increases in capture velocity at an upstream distance equal to the diameter of the hood (11 inches). By increasing capture velocity further from the face, contaminant capture could take place at distances more convenient to the circular slotted-hood operator while maintaining adequate suction. This was to be achieved by the addition of two slots and a flange to a traditional conical hood opening. Three plates were designed to change the geometry of a plain conical hood (slot area: 0.1334, 0.0963 and 0.0694 ft^2). They were tested at different airflow rates (243, 347, 467, 647, 897 cubic feet per minute) for a set number of distances from the hood face using a thermal anemometer. Three-dimensional maps of performance were created for visual comparisons, and t-tests were conducted to analyze performance by comparison of velocity at any point upstream of the hood. Velocity contours illustrated that two of the three designs had greater capture velocities compared to the standalone conical hood, and paired t-tests confirmed the significance ($p<0.05$). Each of the new designs failed to significantly increase capture distance further than 11 inches from the hood. However, increased velocities occurred near the hood opening (within 5 inches). These modest improvements for the largest slot design increases operating pressures by approximately 0.1” wg @ 250 cfm but 1.1” wg @ 650 cfm. Implementing these new designs would increase capture velocities close to the hood, although this advantage is offset by the cost it would require to compensate for the pressure loss incurred.

TABLE OF CONTENTS

LIST OF TABLES

LIST OF FIGURES

CHAPTER I

INTRODUCTION AND LITERATURE REVIEW

Hazardous chemicals are released into the air by countless industrial processes, exposing workers to dangerous levels of toxic materials. In years past, the method for controlling this hazard was using a fan in the general vicinity of each process, with the motto “dilution is the solution”. Diluting the air will not remove these chemical concentrations, simply disperse them. Therefore, it is important to remove the contaminants from the work environment entirely. Preferably, this would be done right at the source, thus minimizing worker exposure. When hazardous materials are generated at a source near a worker, the use of any form of general ventilation, i.e. the use of an exhaust fan as the sole exit for contaminated air, is not acceptable because general ventilation fails to remove the toxicant before the worker is exposed. One method of alleviating this exposure and keeping the workforce safe is adopting the use of local exhaust ventilation.

Local Exhaust Ventilation

Local exhaust ventilation (LEV) are designed systems that prevent the dispersion into the air of dusts, fumes, mists, vapors, and gases in concentrations causing harmful exposure (EOHSS, 2011). Local exhaust ventilation is a primary method for controlling occupational exposures to hazardous airborne contaminants. Local exhaust ventilation is effective at removing contaminants at their source, limiting or eliminating worker exposures altogether (Corteau et al. 2002). Typically LEV hoods are separated into three categories: enclosing, exterior, and receiving (Burgess et al. 2004). Enclosing hoods are the most efficient in controlling contaminate exposure because the process is located inside the hood. A prime example of an enclosing hood is a glovebox. An exterior hood does not surround the contaminant at the point of generation but must be captured at a distance. Movable welding hoods are a common example of an exterior hood. Receiving hoods are more specialized in that they require particle momentum or thermal updrafts for capture. Canopy and grinding wheel hood types are both receiving hoods. Exterior hoods are inherently less satisfactory than enclosing hoods, though the latter is more common in general industry (Burgess et al. 2004). Because exterior hoods are the more common and less efficient option, it is only natural to try and improve the effectiveness of this form of LEV.

There are many operations that employ the use of LEV due to a large proportion of workers being exposed to the dangers of the aerosolized toxic contaminants. The effectiveness of LEV in the workplace has been categorized for numerous industrial processes including: concrete surface grinding (Croteau et al. 2002), welding (Meeker et al. 2007), and even has been used in hairdresser salons (Elihollund et al. 1998). Of these, welding is an industrial process that uses LEV frequently with impressive efficiency. Welding is a common source of exposure to airborne contaminates, especially if performed indoors with no ventilation system in place. According to the Bureau of Labor Statistics, there were 466,400 welders, solderers and brazers in the U.S. though it is believed that over 1 million workers worldwide perform welding as part of their job (BLS, 2008). This is not the only population exposed to these fumes. When no exhaust system is being utilized, the fume will linger and potentially enter breathing zones of other workers in the same plant. A study that looked at manganese (Mn) and total particulate matter (TP) exposures with and without LEV in place found a 75% reduction in Mn and 60% reduction in TP when LEV was used (Meeker et al. 2007). Another study (Liu et al. 2011) that looked at welding fume exposures when LEV was present concluded similar results. Manganese and total particulate matter was measured using a very large data set (N=2065 for TP and N=697 for Mn). The use of LEV lowered the exposure of Mn by 63% and 57% for TP. These reductions in exposure are valuable, though can be furthered by increasing LEV effectiveness. This occupation shows no sign of decline, indicating this hazard will continue to persist if control measures are not employed.

Welding Fume Toxicity

Welding fume contains many chemicals and is entirely dependent on the material being welded. Studies have shown systemic effects of these contaminants ranging from metal fume fever to possible lung cancer formation (Antonini et al. 2003). Some of the chemicals present in the fume are hexavalent chromium, nickel, and manganese. Both hexavalent chromium and nickel are considered human carcinogens when inhaled (Jenkins et al. 2005). Chronic exposures to welding fume can cause increased incidence of pneumonia, bronchitis and is thought to be a risk factor for developing Parkinsonism syndrome (Korczynski, 2000). Manganese is thought to be particularly harmful, having detrimental effects on the nervous system (Flynn, 2009). ACGIH has set a TWA of 0.2 mg/m^3. Even though the Occupational Safety and Health Administration (OSHA) has no permissible exposure limits (PEL) for welding fume, the National Institute for Occupational Safety and Health (NIOSH) and the American Conference of Governmental Industrial Hygienists (ACGIH) both have exposure limits. NIOSH believes metal fume to be an occupational carcinogen (NIOSH, 2005). NIOSH recommends that exposures to welding fume contaminants be reduced to the lowest concentrations technically feasible. ACGIH had set a threshold limit value (TLV) of 5 mg/m^3 as a time-weighted average (TWA) for a normal 8-hour shift during a 40-hour work week (ACGIH, 2001), though in 2004 they removed the TLV for welding fume as a whole and recommended exposures be assessed for each specific chemical present in the fume. Epidemiologic studies have shown a positive correlation of welders having increased frequency and severity of pulmonary infections and overall respiratory illness (Antonini, 2003). Because of these hazards, local exhaust ventilation should be used to control airborne contaminant exposures.

Increasing LEV Effectiveness

The design of the LEV system has much to do with its use and efficiency. There are several different types of LEV hoods designed with capture arms including: plain opening, flanged opening, a conical hood, and a slotted hood. The conical hood is considered the best exterior hood in terms of capture efficiency, the fraction removed over the amount generated (ACGIH 2007). Flanges prevents the airflow from the back of the hood and focus suction straight ahead of the face. A flange is classified by an addition of a rim or disc-shaped collar at the sides around the hood that has a width greater than the square root of the opening area: $w > \sqrt{A}$. The addition of a flange has been shown to increase velocities in front of hoods up to 55% in some cases (Fletcher 1978). Slots are used to create uniform suction over a long surface and are primarily used to increase capture velocity (Fletcher et al. 1982). A slotted hood is classified as an opening with an aspect ratio of width/length > 0.2. Slot hoods create high capture velocities near the hood due to the small area of the opening. Because of this, slot hoods are typically used to exhaust large area sources such as workbench stations or open surface tanks (Conroy et al. 1988). Slot hood capture velocities fall off less rapidly as distances increase from the hood face. Slot hoods have a capture velocity to distance ratio of $1/x$ whereas non-slotted hoods have a ratio of $1/x^2$, where x is the distance upstream of the hood (Burgess et al. 2004). Figure 1 illustrates the geometries of several exhaust hoods previously mentioned.

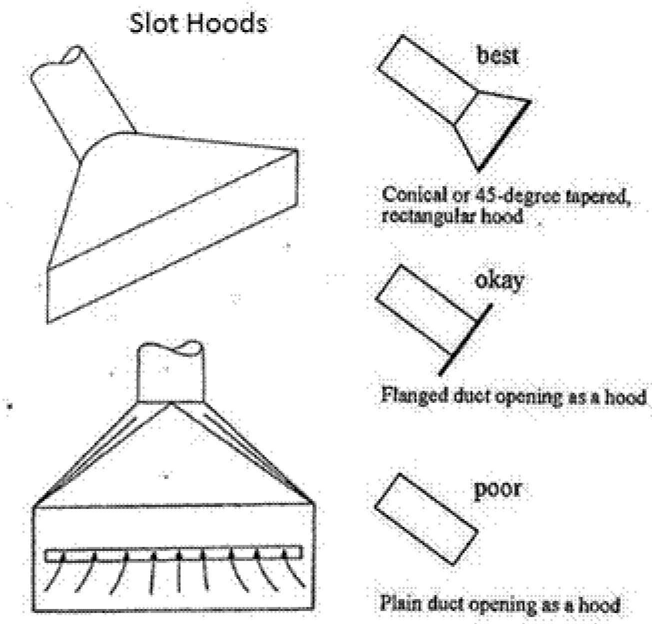

Figure 1. Sample Hood Geometries

A study in Japan looked at creating a circular slot hood that was to be used in a mixing process (Iwasaki et al. 1997). This design was successful in lowering both fine particle counts and organic solvent levels. Another study attempted to lower worker exposures to methylene chloride during furniture stripping used three separate hood configurations to limit these exposures: a slot hood, downdraft hood and a combination of the two (Estill et al. 1996). It was shown that without the use of local exhaust ventilation, the concentrations of methylene chloride ranged from 600-1150 ppm. These values were lowered to 28, 30, and 34 ppm by the combination, the downdraft and the slot hood respectively. This study shows the effectiveness of slot hoods, especially when combined with other exhaust hood geometries. Otherwise, very little information is available on circular slot hoods and their effectiveness. However, this type of design is used in several mobile welding unit hoods. In theory, this design is hypothesized to increase capture velocities by focusing airflow.

Capture velocity is the necessary air velocity at any point upstream of the hood required to overcome opposing air currents, thereby capturing contaminated air (ACGIH, 2007). For contaminated air to be captured, it must be moving at a velocity at or above the capture velocity in order to be drawn into the hood. This value is a good indication of how well a hood performs in terms of capturing contaminates and controlling worker exposures. By increasing capture velocity, the hood effectiveness to capture contaminants is increased likewise.

A typical limitation to the use of local exhaust hoods is the inconvenience of positioning the hood to maximize capture while keeping the hood from getting in the way of the work being performed. This problem would be alleviated if the capture velocity was increased, allowing for increased contaminant capture further from the source of generation.

The focus of this study was to develop and test three slotted circular exterior hoods. Their performance will be compared to that of a similarly dimensional conical hood, where increased velocities upstream of the face are desired for the slot hood.

CHAPTER II

CAPTURE VELOCITY WITH SLOT ENTRY TO CONICAL HOOD

Introduction

Local exhaust ventilation (LEV) systems have been shown to significantly decrease the level of toxic aerosol exposures. During concrete cutting and grinding activities, LEV was shown to significantly ($p<0.05$) decrease the amount of respirable dust exposure (Croteau et al. 2002). LEV was also shown to reduce respirable dust exposure during concrete surface grinding by 92% (Croteau et al. 2004). Placing the hood too far from the source of generation prevents adequate contaminant capture, resulting in increased potential for workers to be exposed to harmful airborne contaminates.

Local exhaust inlets have been tested and improved for many years. The equations derived by Dalla Valle and Silverman to estimate centerline velocities upstream of a hood in the 1930's and 40's are still being used and compared against to this day (Flynn et al., 1988). Their empirically derived equations for estimating velocity along the centerline are the basis for design calculations (Burgess et al., 2007). Dalla Valle characterized circular and rectangular hood openings, while Silverman's work focused on the rectangular slot hood entry. These general equations for estimating velocity along the centerline have been tested against and confirmed by a number of studies (Garrison 1981, Cascetta 1996). As such, these general evaluations of LEV systems, using centerline velocity and their respective distances, are the basis for the work being performed in this study.

The equation developed by Silverman for flanged rectangular slotted hoods to determine velocity any point along the centerline is shown in Equation 1.

$$\frac{V}{V_s} = 0.36 * \left(\frac{x}{w}\right)^{-1} \quad \textbf{(1)}$$

With V being velocity at any point upstream of the hood, V_s is velocity at the slot, x is the distance upstream of the hood and w is the width of the slot.

DallaValle developed the equation for estimating velocity using round flanged hoods that appears as shown in Equation 2:

$$\frac{V}{V_f} = \frac{1}{12.7*\left(\frac{x}{d}\right)^2 + 0.75} \quad \textbf{(2)}$$

With the same terms as above except V_f is the velocity at the hood face.

These equations are used for determining the velocity at any point upstream of the hood, given the location, the hood dimensions and the face/slot velocity given the specific geometry.

Numerous studies use velocity contours to illustrate the performance of particular hood designs (e.g. Ilpo, 1993; Conroy et al., 1989). Velocity contours of flanged hoods show that the addition of a flange to an inlet restricts flow into the hood to locations in front of the opening and allows greater capture velocity in front of the inlet. Slots are typically used to provide uniform airflow across a finite length of contaminant generation, and their effectiveness can be increased with the addition of flanges. (Cascetta and Bellia, 1996). This design feature was explored in this study by including slots and a flange to a conical hood and viewing the resultant increase in velocity.

There are several off-the-shelf systems available that propose to improve contaminant capture compared to the traditional round or flanged-round LEV duct. The Fume-Air™ 750 (Air Systems International, Chesapeake, VA) and the Mobiflex® 200-M (Lincoln Electric, Cleveland, OH) are two welding fume extractors that have differing degrees of round slotted hoods. The Fume-Air™ 750 uses a disc in the center of the hood inlet, creating an uninterrupted circular slot around the perimeter of a round opening. The Mobiflex® 200-M uses a similar perimeter-opening, but it a hexagonal shape for the hood entrance.

We wanted to investigate combining the slot with a flange in an attempt to improve the overall capture velocity. The use of a flange was necessary to focus airflow and increase capture distance further upstream of the face. Also, by limiting the area at which air is pulled through, face velocity would be increased. We theorized the addition of two circular slots would increase upstream velocities as well, in addition to improving uniformity of airflow. By curving the slot around the center of the hood, it would create a “disc” in the center that would focus airflow. Theoretically, the “circular flanged slot-hood” would significantly increase centerline velocities downstream from the hood face.

The goal of this study is to increase capture velocity at distances greater than the diameter of the duct opening. ACGIH shows us that velocity is reduced to approximately 10% of face velocity at one duct diameter away from the opening with minor variations across different hood shapes (ACGIH 2007). Theoretically, extending this critical distance would improve contaminant capture at increased distances from the LEV opening.

Objectives

This study was designed to evaluate whether combining a flanged-slotted entry on to a rounded duct could improve LEV performance. Three objectives were put forth:

1) Determine whether a new design significantly increases capture velocity at one duct diameter upstream of the hood opening. Improvement would be assessed against a conical hood.

2) Determine the relative operation cost of a new design, using static pressure as an indication of performance versus cost.
3) Develop an equation to estimate velocity at any point upstream of the hood for a given slot width and velocity.

Methods

Design Plates

Three designs were created for our slotted conical hood. Plates were created to be able to be placed over a 27.9 cm (11") diameter conical hood (Figure 2). Each plate was a circular disk with a diameter of 29.2 cm (11.5") with the extra half inch added in order to attach the plate to the hood without limiting the face diameter. The plates were made from 1 cm (0.384") thick aluminum with strength as a main concern, assuring that increased pressure from the blower system would not affect the integrity of the plate. Our round slot-hoods had a strip of metal (40° arc) on both sides that holds the center disc in place. In other words, the slot was not continuous. These separations create two slots, each having the same size and shape. Each design was similar in shape with differing slot width (w) and length (l). Plates 2 and 3 were created to follow the rules of a slotted hood (w/l < 0.2) and a flanged hood (flange width > $\sqrt{A}$). Plate 2 required a flange width of 6.69 cm and Plate 3 required 5.68 cm; each were fitted with a flange with a width of 7 cm. Plate 1 had a larger slot area with similar shape and was scaled to the other pates, but exceeded the direct w/l (0.395) and failed to meet the required slot width. Plate 1 required a slot width of 7.87 cm; the available 7 cm flange was insufficient. This plate was to be used as a control rather than an indication of design improvement. The slot areas of Plates 1 through 3 were: 123.97, 89.43 and 64.51 cm^2 (0.1334, 0.0963 and 0.0694 ft^2)

respectively, with between-plate ratios of 1.386. The design specifications are provided in detail in Appendix A.

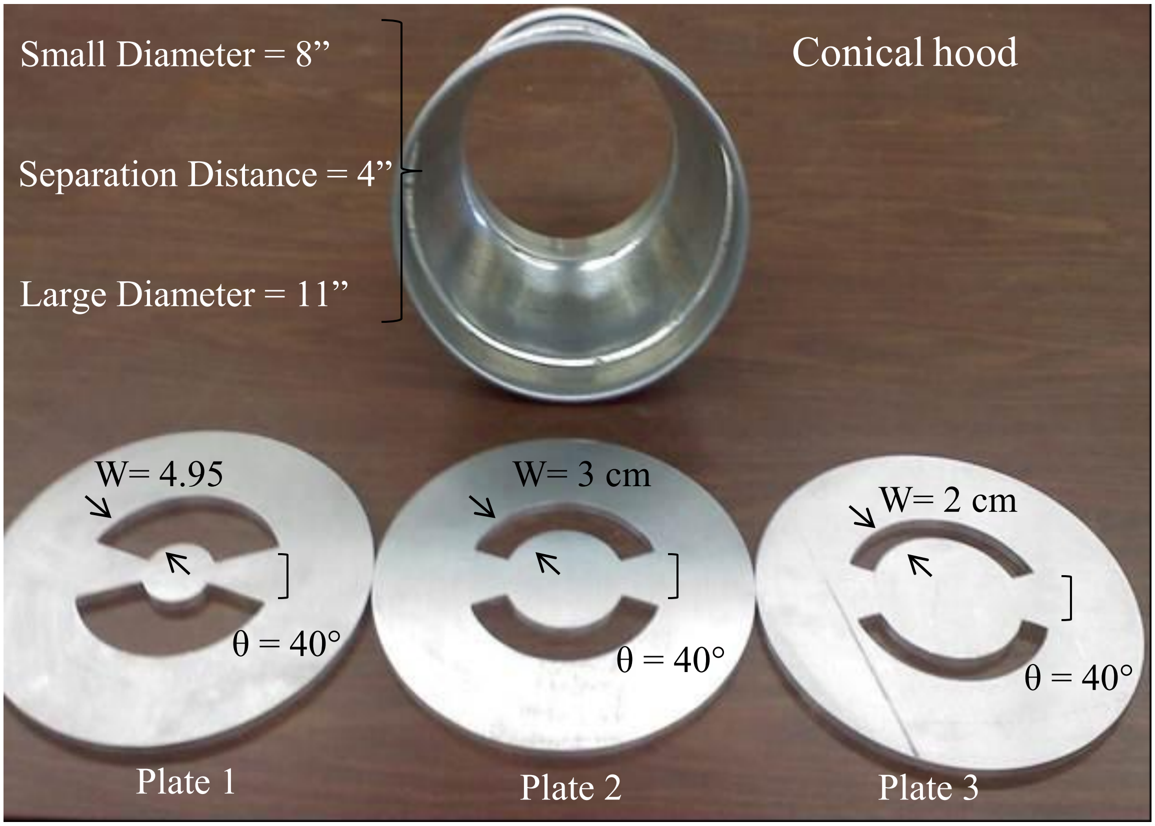

Figure 2. Plate Designs and Conical Hood

Quantifying the System

A 340.4 cm (11’2”) duct system as used as our environmental test model (Figure 3). A six point traverse was used to determine the airflow rate through the system. The six point log-linear method (Burgess et al. 2004) was used to determine these measurement locations within the duct: 0.89, 3.81, 8.89, 19.05, 24.13, and 27.05 cm (0.35, 1.5, 3.5, 7.5, 9.5, and 10.65 inches) from the top wall. The pitot tube was inserted at 40.6 cm (16”) upstream of the blower, at an expanse of 27.9 cm (11”) diameter duct work. This location avoided expansions and contractions, as they may be a source of velocity distortion (Guffey and Booth, 1999). This position followed the traverse location “rule” of the measurement taken at over seven duct diameters away from the opening (300 cm when only 196 cm was required). The velocity pressure readings were in inches of water gauge (in. H_2O) and were converted into velocity readings using Equation 3:

$$V = 4000 * \sqrt{P_v} \quad \textbf{(3)}$$

Where P_v is velocity pressure in inches H_2O and V is velocity in feet per minute (fpm).

These six values were then averaged to find the mean duct velocity. The airflow rate was calculated using Q=VA. Three replicates at each airflow rate were taken. Nine different levels were established from 200-900 cfm. This range gave us a good idea of both the high and low end of the airflow rate spectrum that our motor and fan could achieve with these new inlets. Five airflow rates were chosen based on typical industry rates and to match face velocities between the plates: 243, 337, 467, 647, and 897 cfm. The ratio between airflow rates was the same as the ratio of plate opening areas (1.386) in order to allow comparison of performance by both flow rate and face velocity between plates at different points upstream of the hood. The system was unable to operate at 897 cfm for Plates 2 and 3 or at 647 cfm for Plate 3 due to the large pressure drop. Therefore, 243, 337 and 467 cfm were used to compare all three design plates against the conical hood.

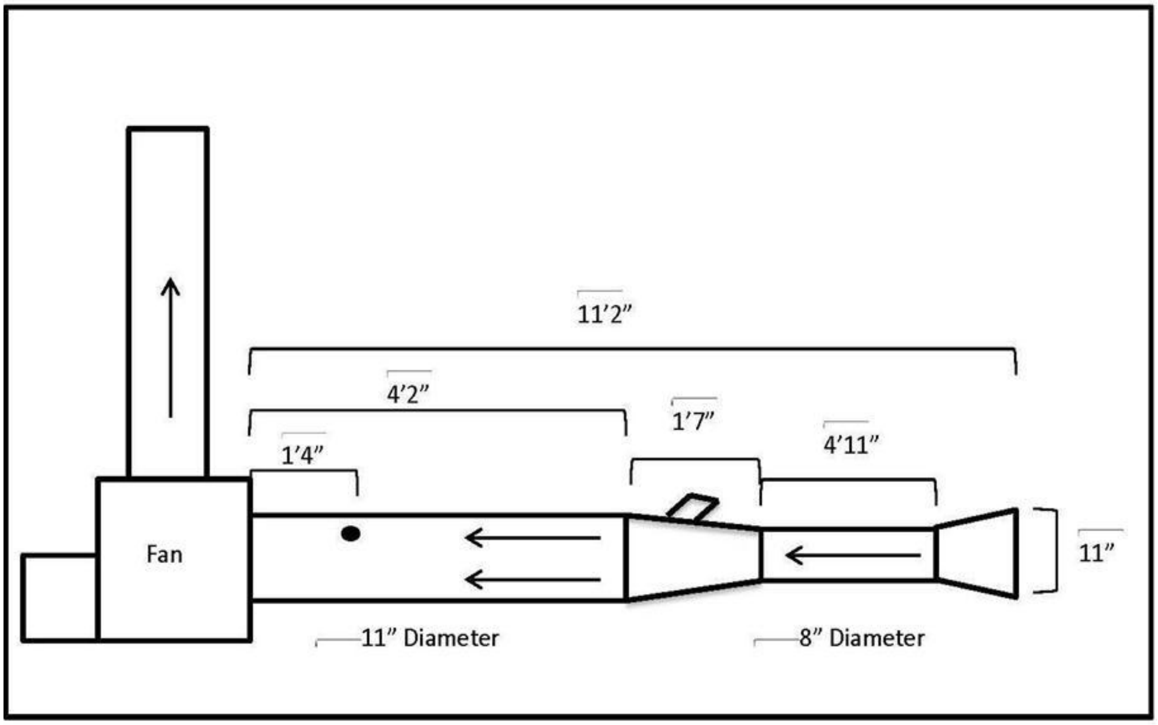

Figure 3. Duct System

The static pressure drop was measured in much the same way as airflow rates were characterized. Pressure drop can be defined as a reduction of pressure at one point of the duct to another, typically downstream to a point upstream. This pressure drop is largely due to frictional losses, though in this case the increase of velocity at the face is causing a large pressure drop right at the hood. The same pitot-tube traverse was performed at the same location, using the same equipment. In this method, instead of collecting velocity pressure measurements, we collected static pressure measurements at all airflow rates for each plate. These static pressure values were then normalized by subtracting the corresponding pressure drop from the pressure drop of the conical hood at a given airflow rate to compare their performance. Thus, the static pressure loss reported is relative to each airflow rate and plate number.

For more information on classifying the blower system see Appendix A.

Downstream Velocity Measurements

A thermal anemometer (VelociCalc® Plus 8386 #02040613 TSI, Inc., Minneapolis, MN) was used to measure air velocity upstream of the hood. These measurements were made along the centerline, the center of each plate extending outwards away from the hood in a straight line. The centerline measurements were taken at the midpoint of the hood at nine positions upstream of each plate up through 34.9 cm (13.75”) from the face (1.25 D). There were more points evaluated closer to the hood, as this is the region of greatest velocity decline, giving us an idea of where the most change occurs and by what magnitude. Three replicate measures of centerline velocity were made for each plate at each of the chosen airflow rates, repositioning the anemometer between each replicate (Table 1).

Table 1. Centerline Distances

Position	Distance from opening (in.)	% Diameter
0	0	0
1	1.1	10
2	2.2	20
3	3.3	30
4	4.4	40
5	5.5	50
6	8.25	75
7	11	100
8	13.75	125

Velocity was also measured off of the centerline, both in horizontal and vertical planes. Distances from the centerline were chosen based on empirically collected upstream preliminary data, at positions velocities would differ noticeably from the centerline. Velocities associated with the three airflow rates of interest for each plate were measured across 39 positions three times each. Five sets of positions were created (Figure 4). These positions were generated by establishing elliptical arcs upstream of the hood entry, with the centerline of a given set at 25, 37.5, 50, 75 and 100% of the duct diameter. The number of measurements each set of data gathered was limited by the distance from the duct face. The further the set was located the more the measurements were taken due to deviations from the centerline having a greater effect at further distances from the hood. The first set of data, with a centerline distance of 25% of the duct diameter, had five measurement points. The second set had seven measurement points, and the final three sets had nine points. This range of distances allowed for spatial comparison and indicated areas of velocity differentiations between plates. Additional information on the location of velocity measurement positions is located in Appendix B.

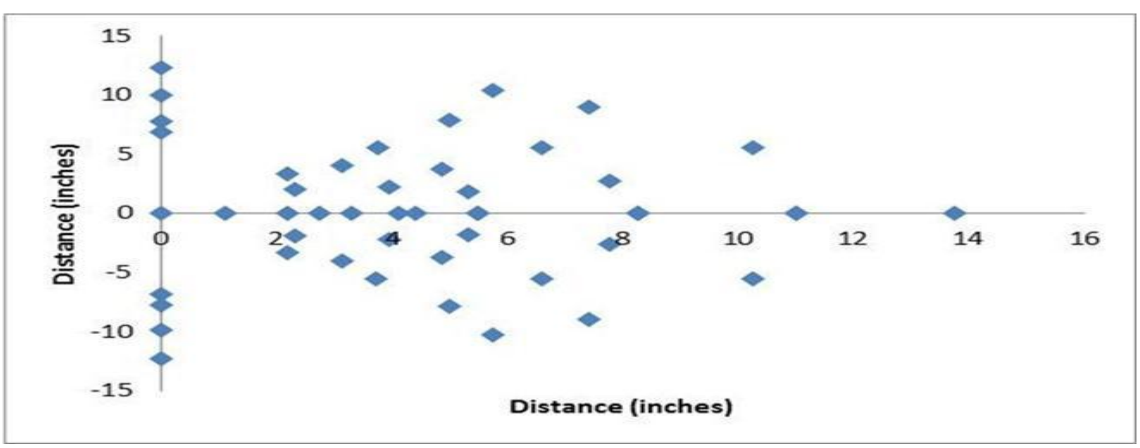

Figure 4. Velocity Measurement Points

Data Analysis

Because the plates are not axisymmetric, differences in velocity between vertical and horizontal positioning of the plate were assessed using paired, two-tailed t-tests. Figure 1 illustrates the solid strip between slots on either side of each plate (θ=40°). This solid area blocked flow and so the position of the plate could, in effect, lower capture velocities. In "horizontal" tests the solid area was oriented as seen in the figure, with the solid strip in the horizontal plane. The "vertical" measures were taken in the same horizontal plane but with the solid strip lying in the vertical plane (rotated 90° from Figure 1).

Three sets of velocity measurements were compared between plates, matching the slot velocities by the ratio of slot areas (1.386). The airflow rates followed this ratio, giving us an indication of between-plate relationships given similar geometries. Pairing these plates together would allow analysis on how velocity was affected upstream of the hood given similar slot velocities. The airflow rates that were paired for a given plate: Plate 1 @ 897 = Plate 2 @ 697 = Plate 3 @ 467, Plate 1 @ 697 = Plate 2 @ 467 = Plate 3 @ 337, Plate 1 @ 467 = Plate 2 @ 337 = Plate 3 @ 243 (all values in cfm). These relationships can be seen in detail in Table 2.

Table 2. Between-Plate Face Velocities

Airflow Rate (CFM)	Conical Hood (FPM)	Plate 1 (FPM)	Plate 2 (FPM)	Plate 3 (FPM)
897	1359	6722	9318	12920
647	980	4849	6722	9319
467	707	3498	4849	6722
337	510	2523	3498	4849
243	368	1820	2523	3498

Downstream velocities were normalized by duct velocity to represent performance improvements over the conical hood and allow comparison between plates. Each velocity measured was divided by the specific duct velocity at that airflow rate (V/V_d). This value would be used in all the comparison tests because it allowed us to compare our slot hood performance with the conical hood. The resultant ratio was then multiplied by 100% to give us a percentage velocity at a certain point in front of the hood compared against the duct velocity. The velocity measurements generated by the above methods were then analyzed both quantitatively and qualitatively. For the qualitative assessment, velocity contours were created so the performance of each plate would be compared visually. The mapping method plotted positions as a percent hood diameter (X/D*100%). This was done using modeling software (Surfer 8, Golden Software Inc., Golden, CO). To quantify between-plate differences in these velocity profiles, paired two-tailed t-tests were performed (Microsoft Excel 2010, Redmond, WA). When testing against the conical hood, paired one-tailed t-tests were performed to identify whether increases in velocity were significant at given distances using an alpha of 0.05. The velocities were compared between plates using velocity data over all positions tested. Comparisons were also made within near and far regions relative to the hood opening to determine whether a specific region had the greatest improvement on capture velocity. This comparison gave us information on whether velocity was significantly increased at a given point upstream of the hood.

Centerline Velocity Equation Development

After the performance of each plate was assessed, each plate was individually evaluated to determine a relationship between centerline velocities, distance upstream from the hood and the slot width. Data was normalized using slot velocity (V/V_S) in order to assess the performance of each plate's slot. This method would allow us to compare our plates with traditional slots and assess any improvement and allow us to create an equation that would estimate centerline velocities at any point in front of the hood given specific design parameters. Linear regression analysis was run on our velocity data and then used for each of the plates to derive an equation to estimate a velocity at any point along the centerline upstream of the hood. Regression was also performed by combining all plate data in order to determine the appropriate single model to estimate centerline velocity. Equation 4 shows the general form of the equation used based on Silverman's slot equation (Eq. 1).

$$\frac{\mathrm{V}}{V_s} = K_1 * \left(\frac{\mathrm{x}}{\mathrm{w}}\right)^{K_2} \quad \textbf{(4)}$$

With V representing velocity at the point upstream of the hood, V_s being the slot velocity, x is the distance upstream of the hood, w is the slot width, K_1 is the intercept, and K_2 is the slope.

Results

Velocity Contours

The velocity contours generated were analyzed and used to visualize the performance of each hood. Figure 4 shows the velocity contours at 467 cfm for all plates. The general shape of the velocity contours for each plate was similar, an ellipse in front of the hood face. However, this ellipse was quite different for each plate design due to the varying hood geometries. Plate 2 and 3 in particular showed a drop in velocity at the centerline close to the hood. This can be attributed to the solid circular region in the middle of the plate. The larger the area of the slot, the smaller the central blockage and the less of an influence this solid area has on velocities. There is a small decrease in velocity near the face of Plate 1 though it disappears rapidly.

These profiles show how quickly the velocity drops off moving upstream of the hood. For example at around 20% the duct diameter, the conical hood velocity falls to 60% of the duct velocity. In contrast, Plate 1 is at approximately 100% of the duct velocity while both Plate 2 and 3 are at 75%. Illustrating how quickly these velocities drop, Plate 1 falls to 30% duct velocity at half a duct diameter upstream of the hood. Figure 5 illustrates that at around 80% of the duct diameter upstream of the hood, all the hoods exhibit nearly identical velocities. Values are given in % duct velocity with the axis having values of % duct diameter. This reporting method helps to establish where the hood placement for specific airflow requirements. (For all velocity contours, see Appendix C).

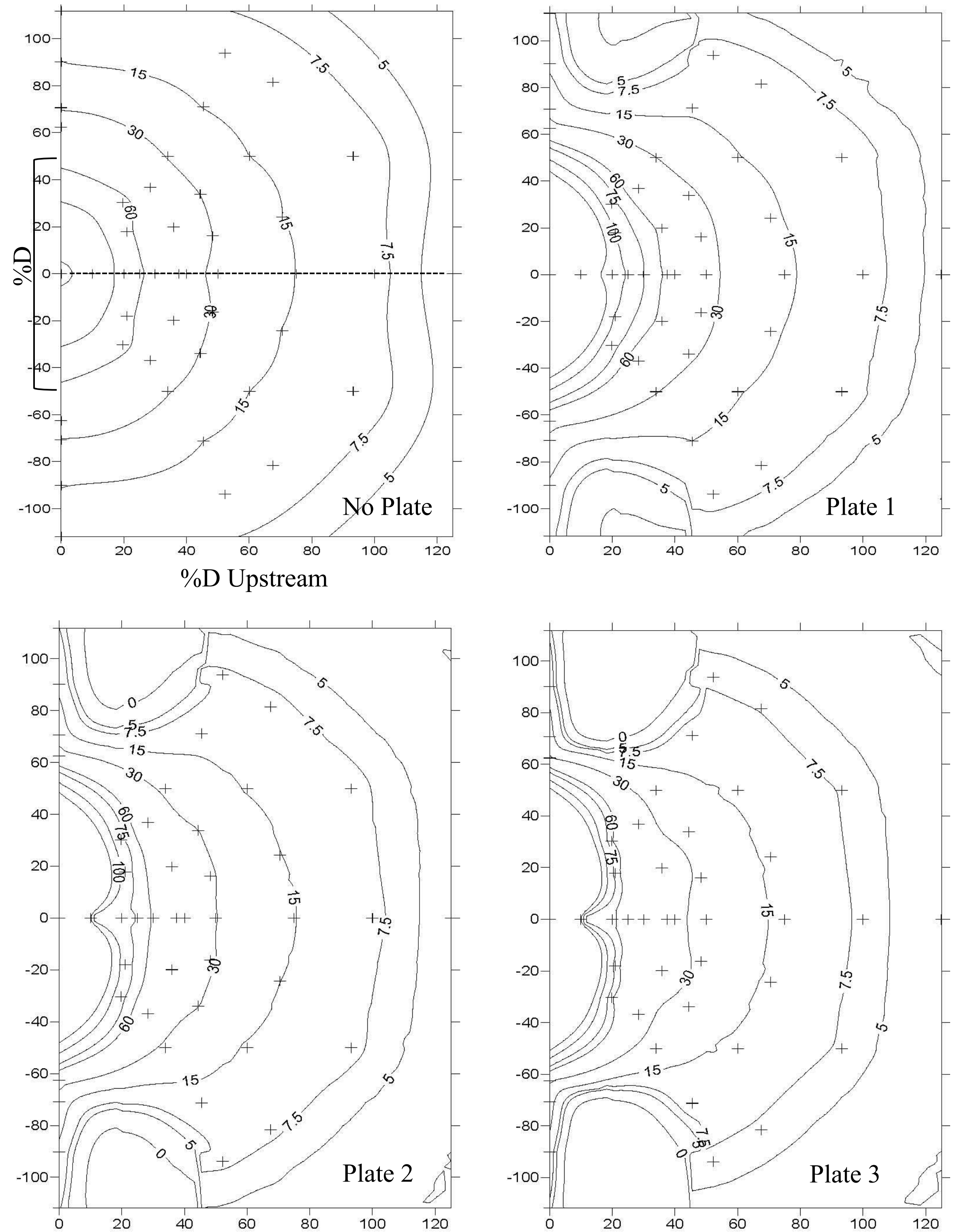

Figure 5. Velocity Contour (467 cfm)

Performance Comparisons

Performance differences between positioning of the plate (horizontal vs. vertical) were a concern because significant differences in capture velocity due to positioning could affect overall capture efficiency and proper usage in the field. Using all the combined horizontal and vertical data, a paired two-tailed t-test was performed between the positioning of the hood and its effect on capture velocities upstream of the hood. These tests showed no statistically significant difference ($p = 0.542$).

Table 3 summarizes the results of the one-tailed, paired t-tests between velocities associated with each plate and the reference conical hood for each plate, showing whether the difference in capture velocity between the plate and the conical opening was significant. In terms of increasing capture velocity upstream of the hood, Plate 1 performed the best of all the plates. Velocity measurements for Plate 1 showed a significant increase in capture velocity over the entire measurement volume ($p < 0.001$). Plate 2, as a whole, was also found to be significantly better than the conical hood ($p = 0.02$). Plate 3 measurement data showed no significant increase in capture velocity over the conical hood ($p = 0.09$).

Table 3. Plate Comparisons Against Conical Hood

Comparisons	All Positions	Effective		Ineffective	
	P-Value	X(cm)	P-Value	X(cm)	P-Value
Plate 1-Conical	< 0.001	≤ 11.4	< 0.001	> 11.4	0.08
Plate 2-Conical	0.02	≤ 5.1	0.04	> 5.1	0.07
Plate 3-Conical	0.09	0	< 0.001	> 0	0.31

For Plate 1, the capture velocity was not significantly more than the conical hood beyond 11.43 cm (4.5”). Closer than 11.43 cm (4.5”), the p-value was <0.001 indicating an increase in capture velocity in this region. From 11.43 to 34.93 cm (4.5-13.75”) the increase in velocity was insignificant ($p = 0.08$). As we increase distances from the face to13.97 cm (5.5”), the improvement becomes insignificant ($p = 0.18$). This result highlights the critical region between statistically improved capture velocities is primarily at close distances upstream of Plate 1.

For Plate 2, velocity was not significantly more than the conical hood past 5.1 cm (2”). Plate 2 showed a significant improvement in capture velocity up through 5.1 cm (2”) upstream of the hood ($p = 0.04$). Beyond 5.1 centimeters (2”), the velocity differences were insignificant ($p = 0.07$). For Plate 3 it was found that velocity was not significantly increased past the hood face. At the slot entry, the increase in velocity was significant ($p << 0.001$). However, upstream of the hood at any distance velocity did not significantly increase ($p = 0.31$). While significant increases in velocity were identified near the hood opening, no plate significantly increased capture velocity at or further than 27.9 cm (11”) from the hood face.

Pressure Drop

Static pressure drop was measured for each plate relative to the conical hood. Figure 6 represents static pressure loss for each plate at a given airflow rate.

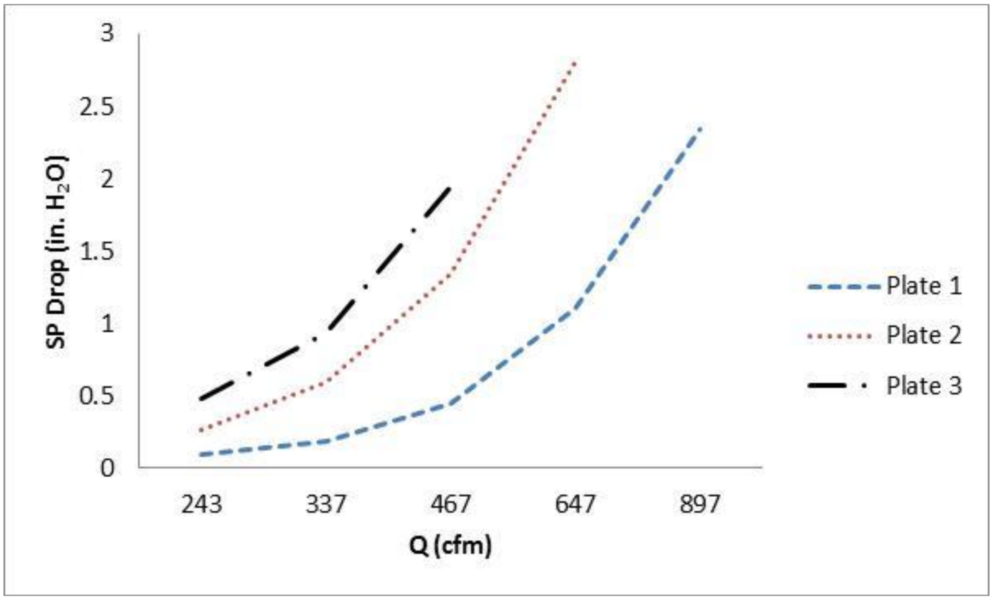

Figure 6. Pressure Drop

Plate 1 had the lowest pressure drop of the three, though at the higher airflow rates it was still substantial. At 243 cfm, the pressure loss incurred was only 0.09" H_20, while at 897 cfm the pressure drop increases to 2.34" H_20. Plate 2 had the second highest pressure drop, and Plate 3 had the largest pressure drop of all three plates.

Centerline Velocity Equation Development

The slot equation was modified to fit our measurement data by using linear regression analysis to determine intercept and slope. The equations that follow in Table 4 are empirically derived modifications of Silverman's rectangular slot equation (Burgess et. al., 2007). When regression was run on each velocity, the slot width along with the distance upstream predicted 82% of the data using the slot velocity equation.

Table 4. Empirically Derived Velocity Prediction Equations

Plate	N	Equation	R^2
Silverman's	-	$\frac{V}{V_s} = 0.36\left(\frac{x}{w}\right)^{-1}$	-
1	350	$\frac{V}{V_s} = 0.26\left(\frac{x}{w}\right)^{-1.5}$	0.875
2	292	$\frac{V}{V_s} = 0.231\left(\frac{x}{w}\right)^{-1.4}$	0.754
3	232	$\frac{V}{V_s} = 0.271\left(\frac{x}{w}\right)^{-1.35}$	0.755
All	874	$\frac{V}{V_s} = 0.241\left(\frac{x}{w}\right)^{-1.37}$	0.821

This data shows that the greatest coefficient of determination belonged to the capture velocity of Plate 1, signifying the greatest ability to predict future outcomes. Plate 1 also had the most negative exponent, i.e. greatest slope, and when combined with the intercept, had the largest velocities at any point. Thus, at the same distance upstream with an increase in slot width, velocity is larger. Plate 2 and 3 had different equations, though fit the model similarly, which has to do with the different slot widths. When all plates were combined to create a velocity prediction equation, 82% of future data can be predicted accurately (Equation 6).

$$\frac{V}{V_s} = 0.241\left(\frac{x}{w}\right)^{-1.37} \qquad \textbf{(6)}$$

Overall, these equations fit well into the modified slot hood equation, allowing us to estimate velocities upstream of the opening for any given circular slotted hood.

Discussion

There were modest improvements to capture velocity with each plate, even though all three plates did not increase velocity at or further than one duct diameter upstream of hood opening. Of the three, Plate 1 with the largest open area was the most promising in terms of actual LEV improvement. It was found that the plate significantly increased capture velocity up through 4.5” (11.43 cm) from the opening but past that, it was no different than the standalone conical hood. This plate’s design did not meet the criteria for slot ($w/l < 0.2$) or flange ($w > \sqrt{A}$) design criteria. Even though the hybrid design of Plate 1 did not meet either specification, it performed better than the conical hood and the circular slotted flange design, and, because the open area was largest, it had minimal pressure drop.

Slots are typically used to provide uniform airflow, not to increase capture velocity (ACGIH 2007). However, because of the unique curvature of the slot on these designs and the flange on the outside, it was theorized to improve capture. The slots on Plate 2 and 3 were too small to be efficiently incorporated into field use, based on the very large pressure drop and minimal velocity improvement with increased velocity only just outside the hood. The slots acted to direct airflow to the opening, but only were successful at these close ranges. The flange effectively focused the airflow from around the sides of the hood to the front, increasing the velocities upstream along the centerline. However, these two additions to the conical hood only increased the capture velocity no more than 2” (5.1 cm) from the hood, while the distances further upstream were unaffected.

The difference was found to be statistically significant between Plate 1 and the other two designs. Plate 2 and 3 had very similar velocity measurements, though Plate 2 performed better in terms of increasing capture velocity upstream of the hood. This finding was expected because Plate 2 and 3 followed the same design parameters, both having slots and flanges. Neither of these two plates were able to significantly increase velocity past 2” (5.1 cm). When this was taken into account with the pressure drop, these two designs showed a lack of efficiency.

Over all upstream positions monitored, the orientation of the plate was found to be statistically insignificant, even though the shape of the plate limited airflow at certain up-close positions. Positioning being unimportant is crucial because workers in the field would not take the time to perfectly align the hood in order to create the most capture, rather it would be positioned at a point of convenience.

Spatial representations using velocity contours allowed us to visualize the performance of each hood. These contour maps showed a similar velocity profile for Plate 1 and the conical hood, with much higher velocities near the hood using Plate 1. Otherwise, the velocity profiles past five inches appear to be similar. Suction falls off rapidly for all designs but this phenomenon was more apparent with Plate 2 and especially Plate 3. Plate 3 has very high velocities immediately by the face, but fall off to the hundreds of feet per minute just inches from the hood (Appendix C). As the airflow rates increase, this dip in velocity near the hood is not as drastic. Each of the new design plates has a velocity restriction along the centerline near the hood, which is more apparent the smaller the slot. This area of lowered velocity is due to the solid "disc" region on each plate. Plate 1 has the least noticeable dip due to the larger slot area which allows velocities to be affected by this obstruction less. There are several strange looking curves in the regions near the hood and away from the centerline, especially noticeable in Plate 3 contours. These regions are areas that velocities were not measured and the software is trying to compensate by creating a velocity curve. This is a limitation of the study, in that data points were limited to what was measured. For future research in this area, it is recommended that more measurements are taken in these regions to tease out any inaccuracies in the modeling software and further the understanding of how these plates behave when deviating from the centerline. Other studies that use contour maps generally are supplying a computer program with an equation and generating data this way (Garrison et al., 1987; Flynn et al. 1989). This study, however, used all collected data in order to accurately represent velocity contours in a real-world setting. Because of that reason, the velocity contours are not exactly curvilinear or symmetrical.

The main problem with the new designs is the amount of pressure drop incurred when operated. The pressure drop relates directly to how hard the fan has to push/pull air and affects the cost of operating the system: the larger the pressure drop, the higher the cost to run the system. As one would expect the smaller the hood opening, the larger the pressure loss incurred. Pressure drop for each hood was considerable, especially at higher airflow rates. This loss of pressure would not be as much of a concern for mobile units or individual hoods but running a duct system with many branches leading to multiple drop down LEV systems would require much more pull from the fan. Practically, pressure loss equates to dollars lost. An essential aspect of designing this hood is not only to improve on capture velocity, but to do so economically. It is important to increase LEV effectiveness while maintaining cost efficiency. The plate that performed the best under these standards was plate 1. At lower air flow rates, the pressure loss was very slight. The big leap in pressure loss was found at approximately 650 cfm. Many units in the field operate at around 500 cfm with others higher and some lower. If this design was applied to the lower range of airflow rates, this pressure drop would be considerably less.

Our derived circular slot equation (eq. 6) varied from the traditional rectangular slot centerline velocity prediction equation (eq. 1). Silverman's slotted velocity equation has an exponent smaller than ours, though the slope is much greater. When calculating velocities along the centerline, the Silverman slot has the larger values. However, Garrison (1981) shows us that the flanged slot actually behaves differently by upstream distance and does not use Silverman's general equation universally. Garrison gives us an equation for close ranges ($0.5 \leq x/w < 1.0$) and far ranges ($1.0 \leq x/w \leq 4.0$) that differ from Silverman's initial equation (Equation 7.1 and 7.2)

$0.5 \leq x/w < 1.0$: $$\frac{V}{Vs} = 0.29\left(\frac{x}{w}\right)^{-0.8} \quad \textbf{(7.1)}$$

$1.0 \leq x/w \leq 4.0$: $$\frac{V}{Vs} = 0.29\left(\frac{x}{w}\right)^{-1.1} \quad \textbf{(7.2)}$$

When the distances are broken down in this manner, our derived equation for the circular slotted hoods has higher velocities at the close range but again has lower velocities at the further distance.

Study Limitations

There are some limitations to the study that may have affected the results. For one, cross drafts could have possibly influenced the velocity readings; especially at distances downstream where hood suction is limited. The measurements were all taken during a time period that no other activity was occurring in the vicinity of the duct system, though rogue airflows from surrounding HVAC systems could have possibly influenced the velocity measurements. Cross drafts should not be seen as a confounder as any work environment these hoods would be used in would have cross drafts, most likely at higher velocities. That being said, the absence or presence of cross drafts should not take away from the studies validity.

Increasing data points both on the centerline and points deviating from it would help refine the study by increasing velocity contour accuracy and centerline velocity estimation. Creating more points away from the centerline would smooth out the velocity contours and give a more accurate representation of where each velocity is experienced. Adding to the nine locations for the centerline measurements would yield better estimation techniques and ability to quantify the specific hood. Also, the addition of more locations along the centerline would allow us to generate a more accurate equation for circular slotted hoods by increasing the R^2 value. Mapping software would be beneficial in further analyzing these plates, by generating points not measured that fit into our model, expanding the results.

The motor on the fan combined with the pressure drops of the plates limited the airflow rates for the smaller slot area plates. Plate 2 and 3 were unable to achieve 897 cfm and Plate 3 was unable to reach 647 cfm. However, using a higher power fan would allow us to get more details into the relationship between plates and how they function at higher velocities.

The addition of a plenum to the slot hood could increase the effectiveness of each design. Plenums are used to regain some of the lost pressure due to the small slot opening. This addition would most likely increase the usability and cost-effectiveness of each hood design. Thus, future studies should look into adding a plenum to the circular slot-hood to determine the applicability.

Conclusion

The purpose of this study was to design a new hood geometry that would increase capture velocity at a duct diameter upstream of the hood. The three hood designs did not improve velocities beyond half a duct diameter. The velocity contours allowed for spatial representations to be accurately depicted and understood, comparing well with published studies using the same mapping method. They showed how alike the new plates behaved as well as the drastic decline in velocity immediately upstream of the hood. Statistical analysis showed us that the orientation of the plate had no significant effect on velocity. This was an important finding as it highlighted the ease of use in the field. Pressure drop associated with each plate offset the advantages of increased velocities near the hood face, though at lower airflow rates this increased cost would be minimal. The empirically derived centerline velocity equations fit the slot model well with an 80% certainty of how future outcomes will be predicted by this model. While this model is not universal due to it only being tested against three differing plates, it does provide a foundation for future work. The results of this study are important to the public health of industrial workers exposed to airborne contaminants because it shows improvement, however modest, on ventilation quality. Though the results were not as impressive as expected, the overall work done leads to follow-up research and development of LEV systems as a whole.

CHAPTER III

CONCLUSION

The round slot hood is efficient at close range, though these improvements to the conical hood decrease with increasing distance from the hood. The main focus of this study was to improve capture distance in order to increase LEV effectiveness. Though this was not achieved, it was found that one new design was able to increase velocities close to the hood with little pressure drop. This modest improvement can be used in applications that require close proximity of the LEV to the source of generation with increased effectiveness. General worker respiratory health would be improved by this new design as it will limit exposures to hazardous materials in a number of industrial processes. Because Plate 1 increased velocities close to the hood with minimal pressure drop, there may be practical applications that come from this study. This may include applying the hood to processes that have a high particle generation rate, cement grinding as an example, that do not require a lot of finesse or mobility of the operator due to the hood placement near the generation. Theoretically it would allow less contaminant escape than the conical hood within 4.5” of the hood, making it appropriate for this type of process. Limiting exposure to fumes and particles released by these processes will ultimately lead to a healthier and more productive workforce.

Future Research

There are opportunities for future research that can be done to further the knowledge base in ventilation technology fields. Following this study, new plate designs using the same criteria could be generated to allow for more diversity in the test group and evidence into why these types of hoods behave in this manner. Choosing plates with the slot and flange criteria met but in different locations would help determine whether it was the addition of the slot/flange or the position that most affected velocities. Because Plate 1 followed neither rule and performed the best, making derivatives of this design may be a better option. Different hood entry diameters would help delineate the witnessed affects and whether they are due to our set up or universal. This would help develop a uniformly applicable capture velocity equation. Altering the angle of the area between slots would affect velocity results and further refine the study. Using different fans to gauge pressure drop against higher or lower airflow rates would also be beneficial. It just might show that even though they are not cost effective at higher airflows, a smaller fan system may work much better with little pressure drop and high velocities.

Holding the pressure drop constant between plate comparisons would allow for a better determination of improvements to performance. By keeping this variable constant the comparability between hood geometries would be increased. This additional comparison variable would allow for a more accurate representation of performance and behavior of the circular slot hood. Also, it would allow us to determine which model performs the best given a particular cost requirement.

The addition of a plenum to the slot hood would help regain some of the energy lost to the slot. Most slot hoods operate with a plenum for that same reason, which may influence our results and increase the effectiveness of each plate. Again, this addition would allow a greater comparison between hood geometries and a more accurate representation of performance.

APPENDIX A: DESIGN SPECIFICATIONS

Table A1 shows the design specifications for all three plates. Each plate had the same outer slot radius with differing inner slot radius to facilitate changes in the slot width and area. Likewise, all outer slot lengths are the same whereas the inner length changes with alterations in slot width. These changes in inner slot length and radius are necessary in order to keep the angle between slots constant. The more the plates are the same, the greater the power for comparison. One can see Plate 2 and 3 follow the slot and flange rule, while Plate 1 fails both. Finally, the ratio between slot areas is shown at the bottom of Table A1, each at 1.386.

Table A1. Plate Design Specifications

	1	2	3
Outer Slot Radius (cm)	7.60	7.60	7.60
Inner Slot Radius (cm)	2.65	4.60	5.60
Slot Width (cm)	4.95	3.00	2.00
Outer Length (cm)	18.57	18.57	18.57
Inner Length (cm)	6.48	11.24	13.68
Slot Length (cm)	12.52	14.91	16.13
Area (cm^2)	61.99	44.72	32.25
Total Area (cm^2)	123.97	89.43	64.51
Total Area (ft^2)	0.13	0.10	0.07
Angle (degrees)	40.00	40.00	40.00
W/L	0.40	0.20	0.12
Flange Required (cm)	7.87	6.69	5.68
Flange (cm)	7.00	7.00	7.00
A1/A2=	1.386		
A2/A3=	1.386		

Figure A1 shows the general plate design. This schematic allowed us to fabricate each plate with the given specifications accurately. Outer slot radius and angle were held constant while inner slot radius was altered in accordance with slot width specifications.

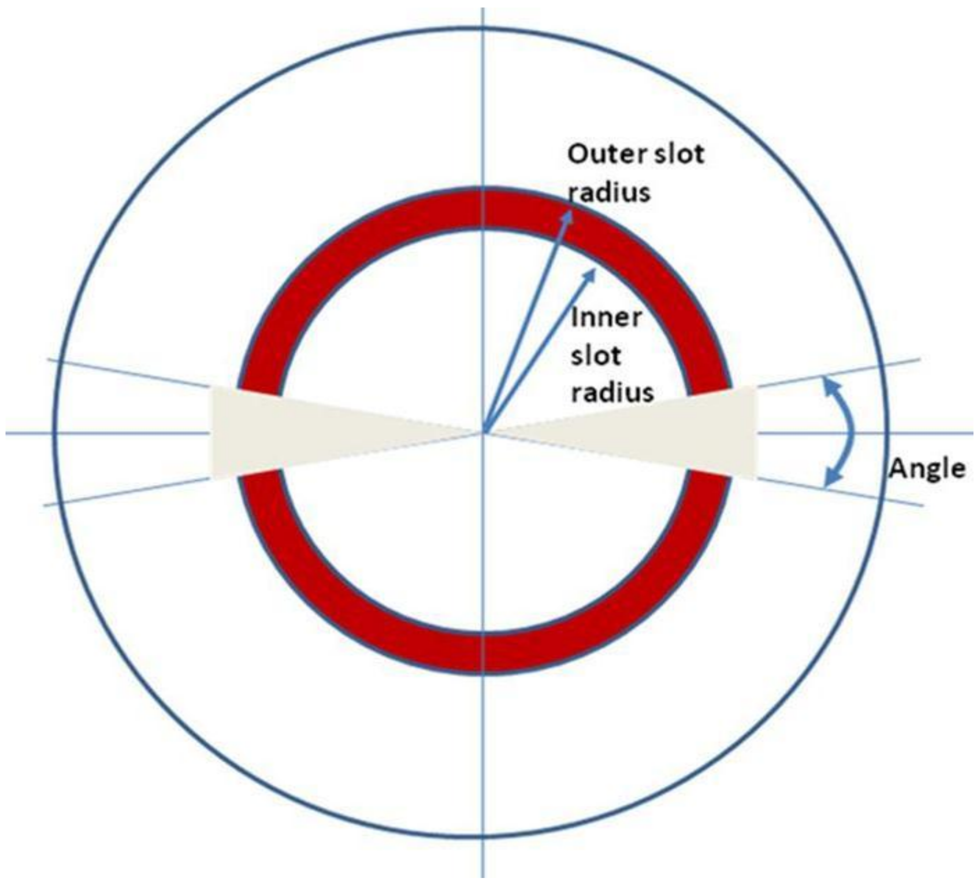

Figure A1. Plate Design Dimensions

Duct System

The duct system used to make measurements was composed of galvanized steel ductwork attached to a single width, single inlet backward curved centrifugal blower (Twin City Fan & Blower BCJ model 105 class 1, serial # 05-212953-1-1). From the blower, the length of the entire duct system was 11’2”. Starting at the blower, the duct had an 11” duct diameter for 4’7”, then tapered to an 8” diameter duct and the hood began at 10’8” down the line. The hood opening was an 11” conical hood that plates could be attached to using special fittings. There were no changes to the overall structure of the duct system between tests.

The duct system had several contractions and expansions that could have possibly altered our results. Though airflow is constant throughout a system, the changes in velocity due to duct area fluctuations could have possibly caused some excess frictional forces and affected our data. Some of the ductwork seemed to be “leaking”, drawing in air from gaps in the fittings. The high pressure drop induced by the smaller slot area plates could have possibly created areas of entry into the duct. This problem was rectified with duct tape.

Figure A2 shows the blower and duct combined system specifications when going from hertz to airflow rate or vice versa. Data points were assigned linear best-fit line that allowed us to develop an equation telling us exactly the amount of power equating to an airflow rate. The equations predicted airflow rates very accurately, with the lowest R^2 value being 0.978 (Plate 2).

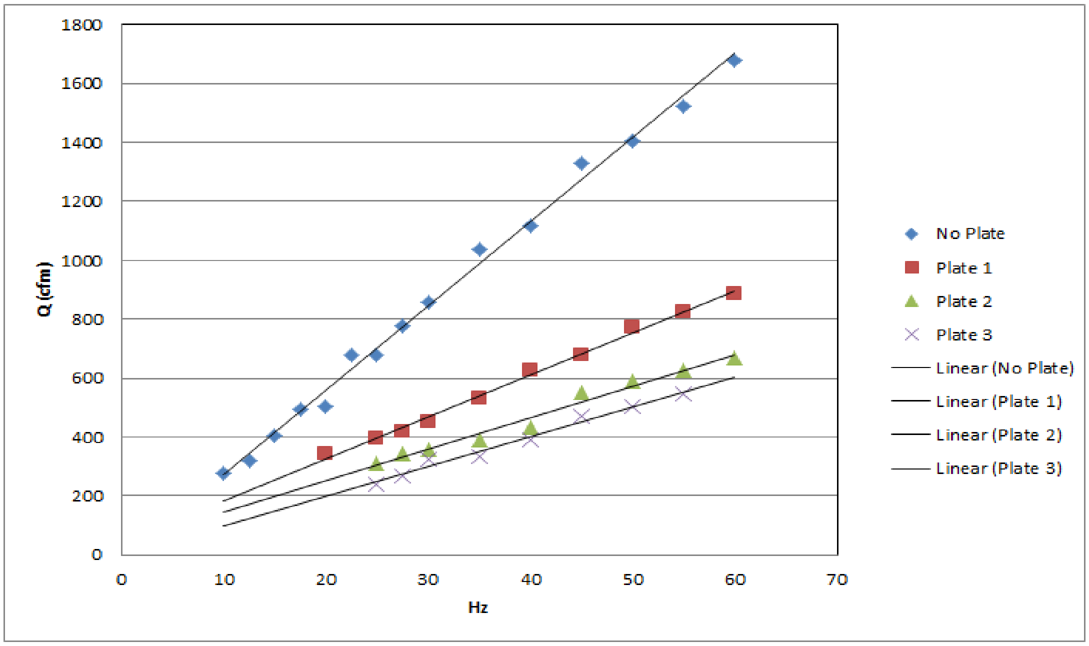

Figure A2. Duct Classification

APPENDIX B: VELOCITY MEASUREMENTS

The goal of this study was to increase capture distance by incorporating a new hood design. This was to be achieved by experimental data collection, including the comparison of velocities (V) between areas (A) of hood designs while holding airflow rate (Q) constant. Our independent variable was A, with Q as our dependent variable and V as our response. There were four levels to the design; plates 1-3 and the standard conical hood. The treatments to the experiment were the distances from the hood face. These distances were decided by the ratio of distance from hood to hood diameter.

Table B1 shows the exact locations of each measuring point in terms of the x and y axis. Distances in the y plane are deviations from the centerline; negative numbers represent below the centerline and positive values indicate above the centerline, depending upon the orientation of the plate. X positions are distances upstream of the hood, along the centerline.

Table B1. Set Distances Outside Centerline

Set	Point ID	Upstream Position (X), Inch	Lateral Position (Y), Inch
1	1	2.17	-3.33
	2	2.31	-1.97
	3	2.75	0
	4	2.31	1.97
	5	2.17	3.33
2	1	0	-6.88
	2	3.12	-4.05
	3	3.95	-2.19
	4	4.13	0
	5	3.95	2.19
	6	3.12	4.05
	7	0	6.88
3	1	0	-7.78
	2	3.74	-5.5
	3	4.88	-3.73
	4	5.31	-1.78
	5	5.5	0
	6	5.31	1.78
	7	4.88	3.73
	8	3.74	5.5
	9	0	7.78
4	1	0	-9.92
	2	5	-7.83
	3	6.61	-5.5
	4	7.76	-2.67
	5	8.25	0
	6	7.76	2.67
	7	6.61	5.5
	8	5	7.83
	9	0	9.92
5	1	0	-12.3
	2	5.75	-10.32
	3	7.43	-8.97
	4	10.25	5.5
	5	11	0
	6	10.25	5.5
	7	7.43	8.97
	8	5.75	10.32
	9	0	12.3

Measurement Devices

A pitot tube was used as our primary standard. Pitot tubes can be used to determine three different values: the total pressure, static pressure and velocity pressure. The pitot tube is positioned to point upstream and parallel to the airflow. All other devices used were calibrated by the pitot tube before each experimental data collection. An inclined manometer was used to measure pressures within the duct system and determine the air flow rates used for each plate. The manometer was also used to determine static pressure drop, which is an indication of how hard the fan has to work and the resultant cost of operation. The manometer was used because it is the simplest and most reliable pressure indicator used in conjunction with the pitot tube (Burgess et al., 2004).

For the velocity measurements, a thermal anemometer was used. Thermal anemometers use a heated element to determine velocities by the rate of cooling an airstream causes the element; the rate of cooling is proportional to the velocity of the air flow. This particular device is good for measuring velocities between 0-10,000 feet per minute (TSI, Shoreview MN). The thermal anemometer is known to have great sensitivity at lower velocities, so this device was perfect for our purposes. Also, the thermal anemometer standardizes the readings so temperature and pressure calculations can be omitted. Table B1 represents the raw data gathered and transformed data. Pictured is only a small representation of a much larger data set. This table is a small portion of Plate 1's velocity and distance measurements at 897 cfm.

Table B2. Snapshot of Velocity Measurement Data

Plate	Q	String	Position	X	Y	V	% D (X)	V/Vo	V/Vo (%)	% D (Y)
1	897	1	1	2.17	-3.33	1035	19.7	0.761484	76.14838	-30.2727
1	897	1	2	2.31	-1.97	1245	21.0	0.915988	91.59878	-17.9091
1	897	1	3	2.75	0	1310	25.0	0.96381	96.38104	0
1	897	1	4	2.31	1.97	1225	21.0	0.901273	90.12731	17.90909
1	897	1	5	2.17	3.33	995	19.7	0.732054	73.20545	30.27273
1	897	1	1	2.17	-3.33	1060	19.7	0.779877	77.98771	-30.2727
1	897	1	2	2.31	-1.97	1280	21.0	0.941738	94.17384	-17.9091
1	897	1	3	2.75	0	1315	25.0	0.967489	96.74891	0
1	897	1	4	2.31	1.97	1275	21.0	0.93806	93.80597	17.90909
1	897	1	5	2.17	3.33	1015	19.7	0.746769	74.67691	30.27273
1	897	1	1	2.17	-3.33	1025	19.7	0.754126	75.41265	-30.2727
1	897	1	2	2.31	-1.97	1275	21.0	0.93806	93.80597	-17.9091
1	897	1	3	2.75	0	1370	25.0	1.007954	100.7954	0
1	897	1	4	2.31	1.97	1210	21.0	0.890237	89.02371	17.90909
1	897	1	5	2.17	3.33	1030	19.7	0.757805	75.78051	30.27273
1	897	2	1	0	-6.875	486	0.0	0.357566	35.75663	-62.5
1	897	2	2	3.12	-4.05	625	28.4	0.459833	45.98332	-36.8182
1	897	2	3	3.95	-2.1857	775	35.9	0.570193	57.01932	-19.87
1	897	2	4	4.13	0	795	37.5	0.584908	58.49078	0
1	897	2	5	3.95	2.1857	775	35.9	0.570193	57.01932	19.87
1	897	2	6	3.12	4.05	630	28.4	0.463512	46.35119	36.81818
1	897	2	7	0	6.875	466	0.0	0.342852	34.28516	62.5
1	897	2	1	0	-6.875	476	0.0	0.350209	35.0209	-62.5
1	897	2	2	3.12	-4.05	620	28.4	0.456155	45.61545	-36.8182
1	897	2	3	3.95	-2.1857	745	35.9	0.548121	54.81212	-19.87
1	897	2	4	4.13	0	815	37.5	0.599623	59.96225	0
1	897	2	5	3.95	2.1857	785	35.9	0.577551	57.75505	19.87
1	897	2	6	3.12	4.05	630	28.4	0.463512	46.35119	36.81818
1	897	2	7	0	6.875	470	0.0	0.345795	34.57946	62.5
1	897	2	1	0	-6.875	484	0.0	0.356095	35.60948	-62.5
1	897	2	2	3.12	-4.05	635	28.4	0.467191	46.71905	-36.8182
1	897	2	3	3.95	-2.1857	745	35.9	0.548121	54.81212	-19.87
1	897	2	4	4.13	0	810	37.5	0.595944	59.59438	0
1	897	2	5	3.95	2.1857	770	35.9	0.566515	56.65145	19.87
1	897	2	6	3.12	4.05	650	28.4	0.478227	47.82265	36.81818

Centerline Velocity Equation Development

For every type of hood, there have been equations derived that allow us to calculate velocity at any distance away from the hood along the centerline. Flanged hoods and slotted hoods have been characterized by this method as well. Therefore, it was important to gather enough data to be able to confidently develop an equation that characterizes our new hood design. This process was done using a linear regression model. Typical hood types use the hood diameter as a prediction variable, and slotted hoods use the slot width. We were unsure as to which dimension would be more accurate in prediction of velocity so we tested both variables and compared their R^2 values. The equations chosen to be used were:

$$\frac{V}{V_s} = K_1 * \left(\frac{x}{w}\right)^{K_2} \qquad \textbf{(4)}$$

and

$$\frac{V}{V_f} = K_1 * \left(\frac{x}{d}\right)^{K_2} \qquad \textbf{(5)}$$

Depending on whether slot width (4) or duct diameter (5) was to be used where K_1 is our intercept, K_2 is our slope, V_s is slot velocity, V_f is face velocity, x is the centerline distance from the hood, w is the slot width and d is the hood diameter.

Linear regression analysis was run on each set of velocities, in order to determine which variable, slot width or duct diameter, estimated our velocity measurements better. In order to perform linear regression on our velocity data, the measurements needed to be transformed. We needed to fit Equation 4 and 5 into the format linear regression accepts (y=b+mx). The natural log of $\frac{V}{V_s}$ or $\frac{V}{V_f}$ was taken to get our “y” value for the regression model. Again, the natural log of $\frac{x}{w}$ or $\frac{x}{d}$ was taken to get our “x” value, depending on which parameter we were testing. Finally, the natural log of K_1 was “b” and K_2 was “m”. In this format we were able to run linear regression on our data and determine fit for each individual plate’s set of velocities and a combined all plates data set. This analysis also gave us an intercept and slope we could transform back into our chosen models (eq. 4 & 5) in order for comparison with already developed slot velocity equations (eq. 1) and for future estimation of the circular slot hood performance. K_2 fit directly into our model with no transformation required, while K_1 had to be modified by taking e^{K1} for it to fit back into our equations. Once these transformations were accomplished, complete equations for centerline velocity estimation were generated for each plate individually and as a set. The R^2 values would tell us which model fit best and would determine which set of variables was the best in terms of velocity prediction along the centerline. It was important to acquire the best predictor of velocity along the centerline so that future work could be done with similar results using the circular, slotted conical hood.

APPENDIX C: VELOCITY CONTOURS

Velocity contours C1-4 are representative of airflow rates of 243, 337, 647 and 897 cfm. 467 cfm is pictured in the text (Figure 4). All contour maps follow the same scale and represent both horizontal and vertical plane data sets.

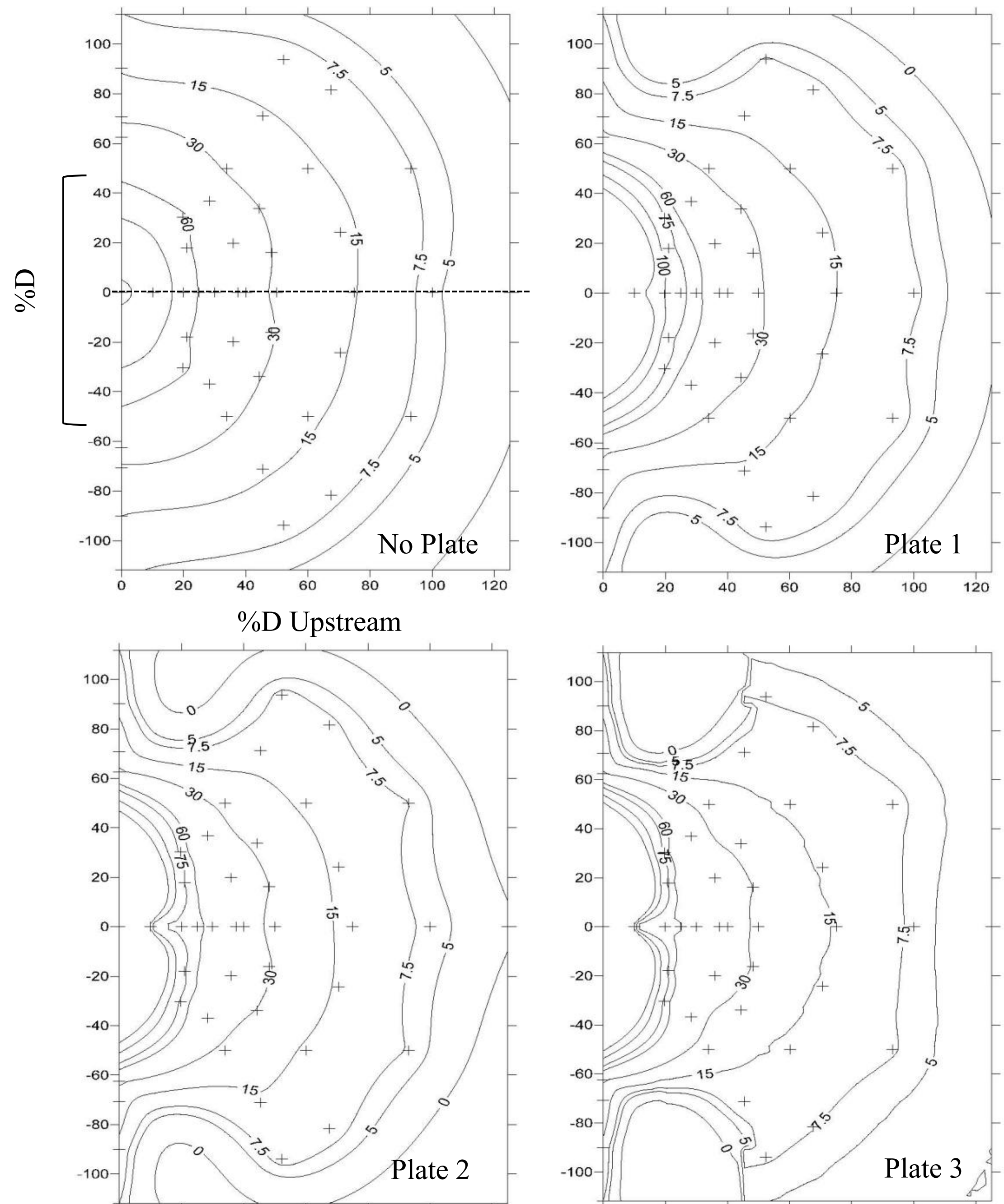

Figure C1. Velocity Contour (243 cfm)

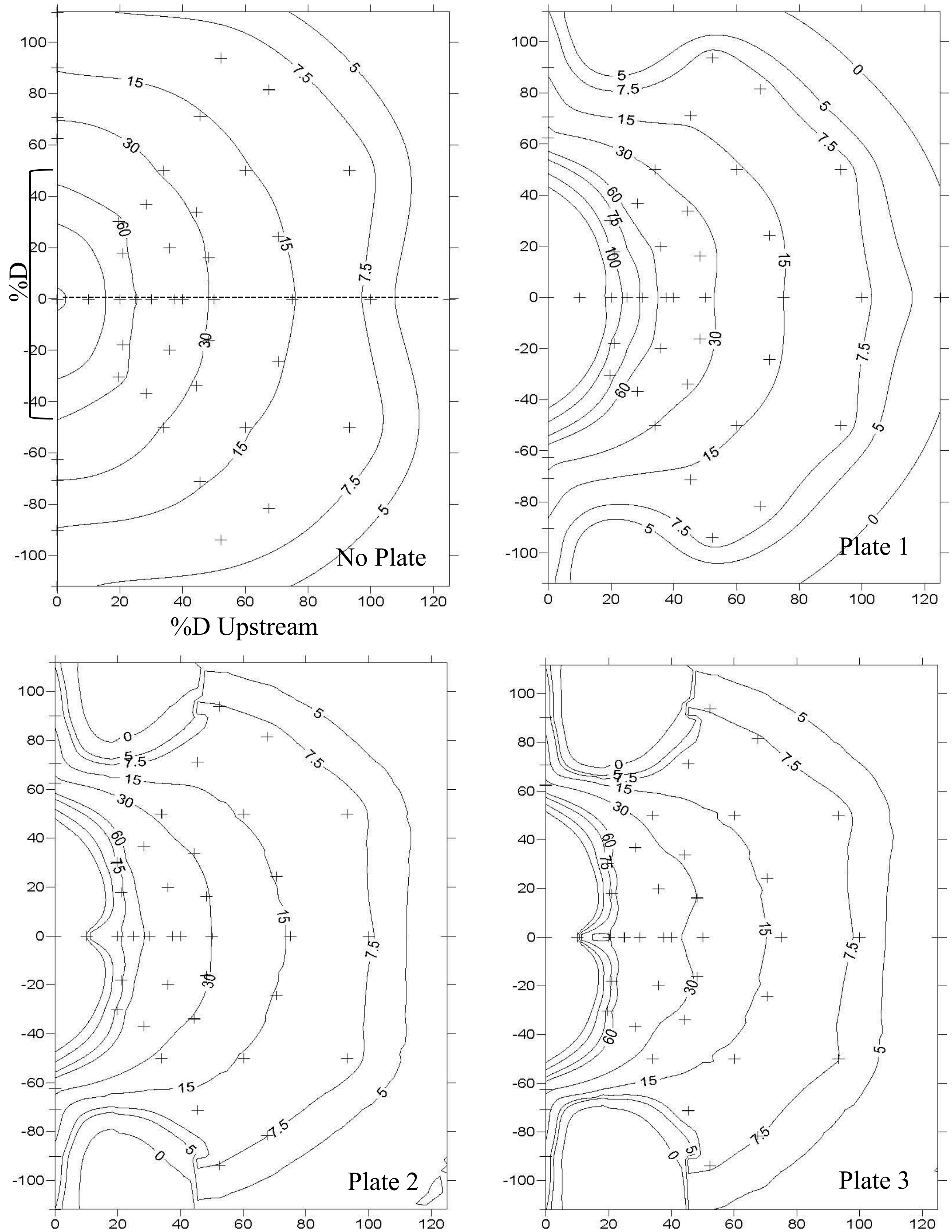

Figure C2. Velocity Contour (337 cfm)

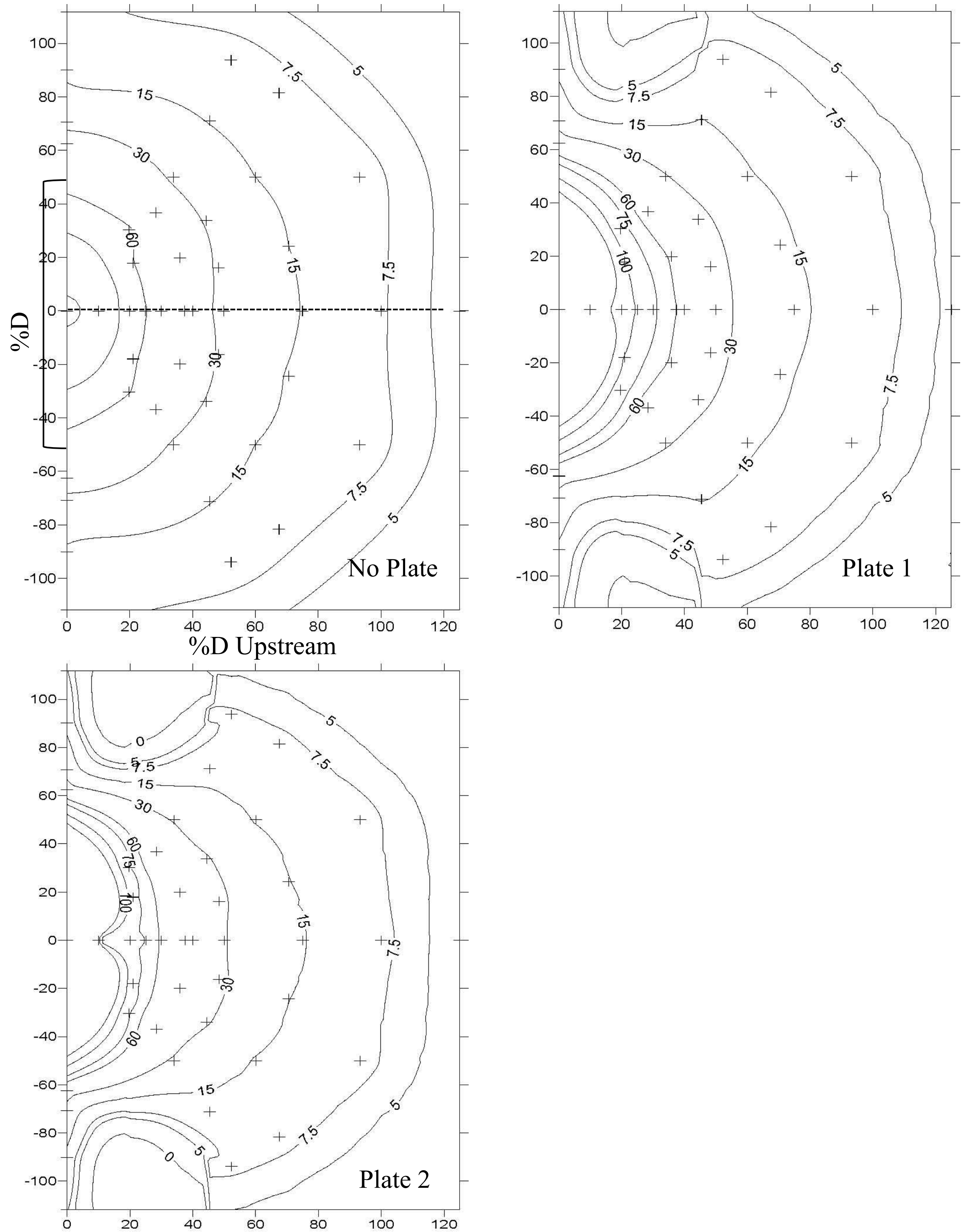

Figure C3. Velocity Contour (647 cfm)

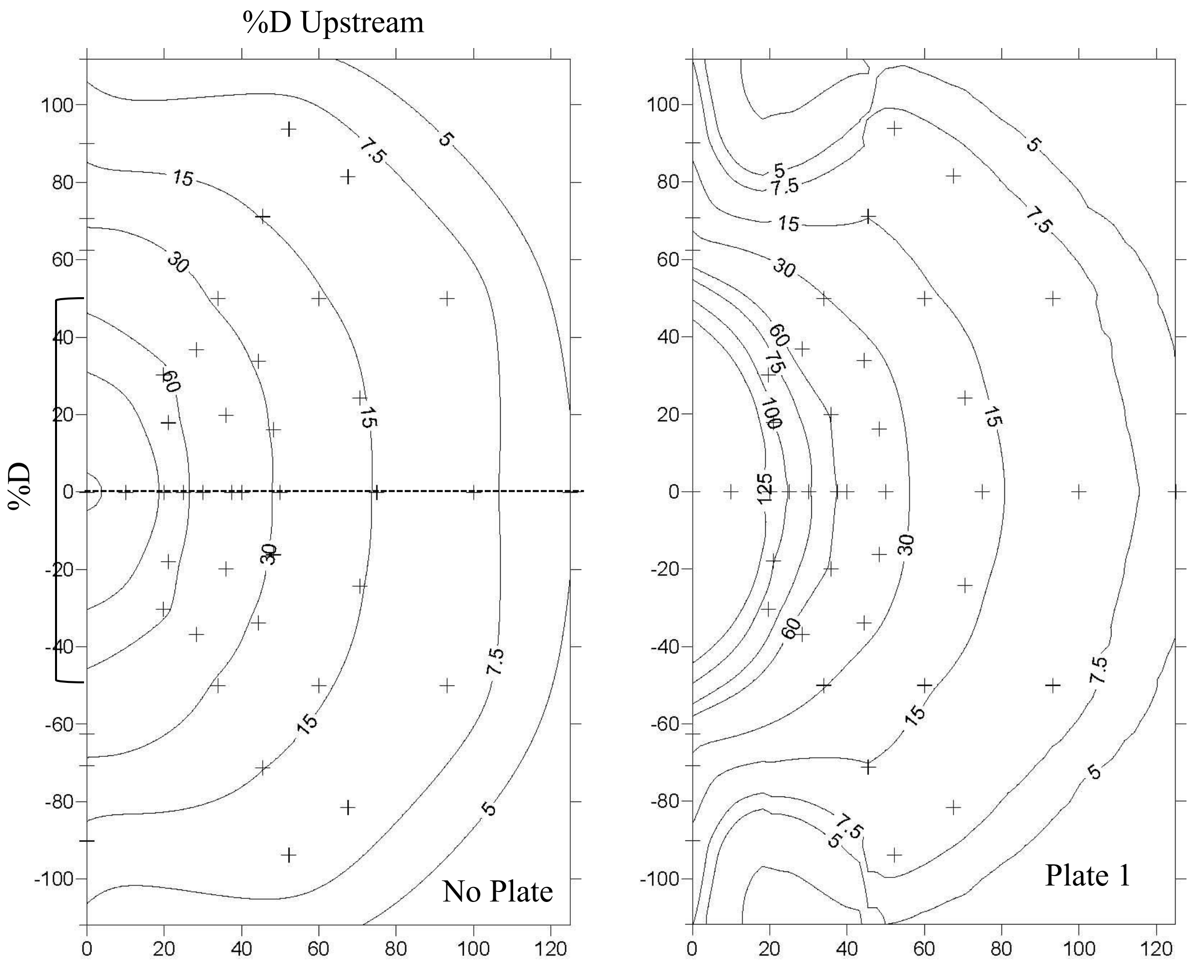

Figure C4. Velocity Contour (897 cfm)

REFERENCES

Air Systems International. Portable HEPA welding fume extractors. Retrieved 12/10, 2010, from http://www.airsystems.com/product_pages/environmental_control/portable_fume_extractor.htm

American Conference of Governmental Industrial Hygienists, Committee on Industrial Ventilation: *Industrial Ventilation – A Manual of Recommended Practice*. 26th Ed. Cincinnati, OH (2007)

American Conference of Governmental Industrial Hygienists (2001). *Threshold Limit Values for Chemical Substances and Physical Agents.* Retrieved 12/13, 2010, from http://www.acgih.org/TLV/

Antonini, J. M. (2003). Health effects of welding. *Critical Reviews in Toxicology,* 33 (1), 61-103.

Antonini, J. M., Lewis, A. B., Roberts, J. R. and Whaley, D. A. (2003). *Pulmonary* Effects of welding fumes: review of worker and experimental animal studies. *American Journal of Industrial Medicine*, 43, 350-360.

Bureau of Labor Statistics (2008). *Welding, Soldering and Brazing Workers*. Retrieved 1/15, 2011, from http://www.bls.gov/oco/ocos226.htm

Burgess, W. A., Ellenbecker, M. J., Treitman, R. D. (2004). Ventilation for control of the work environment (2nd ed.). New Jersey: John Wiley & Sons, Inc.

Cascetta, F., (1996). Experimental evaluation of the velocity fields for local exhaust hoods with circular and rectangular openings. *Building and Environment*, 31 (5), 437-449.

Cascetta, F., Bellia, L., (1996). Velocity fields in proximity of local exhaust hood openings: an intercomparison between current recommended formulas and experimental studies. *Building and Environment*, 31 (5), 451-459.

Conroy, L. M., Ellenbecker, M. J., Flynn, M. R. (1988) Prediction and measurement of velocity into flanged slot hoods. *American Industrial Hygiene Association Journal*, 49 (5), 226-223.

Conroy, L. M., Ellenbecker, M. J. (1989). Capture efficiency of flanged slot hoods under the influence of a uniform cross draft: model development and validation. *Applied Industrial Hygiene*, 4 (6), 135-142.

Croteau, G. A., Guffey, S.E., Flanagan, M.E., Seixas, N.S. (2002). The effect of local exhaust ventilation controls on dust exposures during concrete cutting and grinding activities. *American Industrial Hygiene Association Journal,* 63(4), 458-467.

Croteau, G. A., Guffey, S.E., Flanagan, M.E., Seixas, N.S., Camp, J.E. (2004). The efficacy of local exhaust ventilation for controlling dust exposures during concrete surface grinding. *American Industrial Hygiene Association Journal,* 48 (6), 509-518.

Dalla Valle, J. M. (1939). Principles of hood design. USHS, Washington DC.

Elihollund, B., Moen, B. (1998). Chemical exposures in hairdresser salons: effect of local exhaust ventilation. *Annals of Occupational Hygiene*, 42 (4), 277-281.

Ellenbecker, M. J., Sc. D., Gempel, R. F., Burgess, W. A. (1983). Capture efficiency of local exhaust ventilation systems. *American Industrial Hygiene Association Journal,* 44(10), 752-755.

Estill, C. F., Spencer, A. B. (1996) Case study: control of methylene chloride exposures during furniture stripping. *American Industrial Hygiene Association Journal,* 57 (1), 43-44.

Fletcher, B. (1978). Effect of flanges on the velocity in front of exhaust ventilation hoods. *Annals of Occupational Hygiene,* 21 (3), 265-269.

Fletcher, B., Johnson, A. E. (1982). Velocity profiles around hoods and slots and the effects on the adjacent plane. *Annals of Occupational Hygiene,* 25 (4), 365-372.

Flynn, M. R., Susi, P. (2009). Manganese, iron, and total particulate exposures to welders. *Journal of Occupational and Environmental Hygiene*, 7 (2), 115-126.

Flynn, M. R., Miller, C. T. (1989). The boundary integral equation method (BIEM) local exhaust hood flow fields. *American Industrial Hygiene Association Journal*, 50 (5), 281-288.

Flynn, M. R., Miller, C. T. (1988). Comparison of models for flow through flanged and plain circular hoods. *The Annals of Occupational Hygiene*, 32(3), 373-384.

Flynn, M. R., Ellenbecker, M. J. (1985). The potential flow solution for air flow into a flanged circular hood. *American Industrial Hygiene Association Journal*, 46 (6), 318-322.

Garrison, R. P., (1981). Centerline velocity gradients for plain and flanged local exhaust inlets. *American Industrial Hygiene Association*, 42 (10), 739-746.

Garrison, R. P., (1983). Velocity calculation for local exhaust inlets – empirical design equations. *American Industrial Hygiene Association*, 44 (12), 937-940.

Garrison, R. P., Wang,Y. (1987). Finite element application for velocity characteristics of local exhaust inlets. *American Industrial Hygiene Association Journal*, 48 (12), 983-988.

Guffey S. E., Booth D. W. (1999). Comparison of pitot traverses taken at varying distances downstream of obstructions. *American Industrial Hygiene Association Journal*, 60 (2), 165-74.

Ilpo, K. (1993). Numerical calculation of air flow field generated by exhaust openings. *Annals of Occupational Hygiene*, 37 (5), 451-476.

Iwasaki, T., Ojima, J. (1997). Design of a circular slot hood for a local exhaust system and its application to a mixing process for fine particles and organic solvents. *Industrial Health,* 35 (1), 135-142.

Jenkins, N. T., Eagar, T. W. (2005). Chemical analysis of welding fume particles. *Welding Journal*, 84 (6), 87-93.

Korczynski, R. E. (2000). Occupational health concerns in the welding industry. *Applied Occupational and Environmental Hygiene,* 15 (12), 936-945.

Kulmala, I. K. (1997). Air flow field near a welding exhaust hood. *Applied Occupational and Environmental Hygiene*, 12 (2), 101-104.

Lincoln Electric Company. Mobiflex® 200-M and 400-MS. Retrieved 12/10, 2010, from http://content.lincolnelectric.com/pdfs/products/literature/e1312.pdf

Liu, S., Hammond, S. K., Rappaport, S. M. (2011). Statistical modeling to determine sources of variability in exposures to welding fumes. *Annals of Occupational Hygiene,* 55 (3), 305-318.

Meeker, J. D., Susi, P. Flynn, M. R. (2007). Manganese and welding fume exposure and control in construction. *Journal of Occupational and Environmental Hygiene*, 4 (12), 943-951.

National Institute of Occupational Safety and Health (2005). *NIOSH pocket guide to chemical hazards*. Retrieved 12/13, 2010, from http://www.cdc.gov/niosh/npg/npgd0666.html

TSI Incorporated. VelociCalc® Plus multi-parameter ventilation meters. Retrieved 4/4, 2011, from http://www.tsi.com/uploadedFiles/Product_Information/Literature/Spec_Sheets/VCALpl.pdf

TumSuden, K. D., Flynn, M. R., Goodman, R. (1990). Computer simulation in design of local exhaust hoods for shielded metal arc welding. *American Industrial Hygiene Association Journal*, 51(3), 115-126.

University of Medicine and Dentistry of New Jersey. Environmental and Occupational Health and Safety Services. Retrieved 5/9, 2011, from http://www.umdnj.edu/eohssweb/publications/glossary3.htm

Wallace, M., Fischbach, T. (2002). Effectiveness of local exhaust for reducing welding fume exposure during boiler rehabilitation. *Applied Occupational and Environmental Hygiene*, 17 (3), 145-151.